Supplementary Information

Porous CuO Nanotubes/Graphene with Sandwich Architecture as High-performance Anodes for Lithium-ion Batteries

Shuning Xiao,[ab] Donglai Pan,[a] Liangjun Wang,[c] Zhengzhong Zhang,[a] Zhiyang Lyu,[b] Wenhao Dong,[b] Xiaolang Chen,[a] Dieqing Zhang,*[,a] Wei Chen*[,abc] and Hexing Li *[,a]

a Education Ministry Key Lab of Resource Chemistry, Shanghai Key Laboratory of Rare Earth Functional Materials, International Joint Lab of Resource Chemistry SHNU-NUS-PU, Department of Chemistry, Shanghai Normal University, Shanghai 200234, China.

b Department of Chemistry, National University of Singapore, 3 Science Drive 3, 117543, Singapore.

c Department of Physics, National University of Singapore, 2 Science Drive 3, 117542, Singapore.

E-mail: Dieqing Zhang, dqzhang@shnu.edu.cn; Hexing Li, Hexing-li@shnu.edu.cn; Wei Chen, phycw@nus.edu.sg.

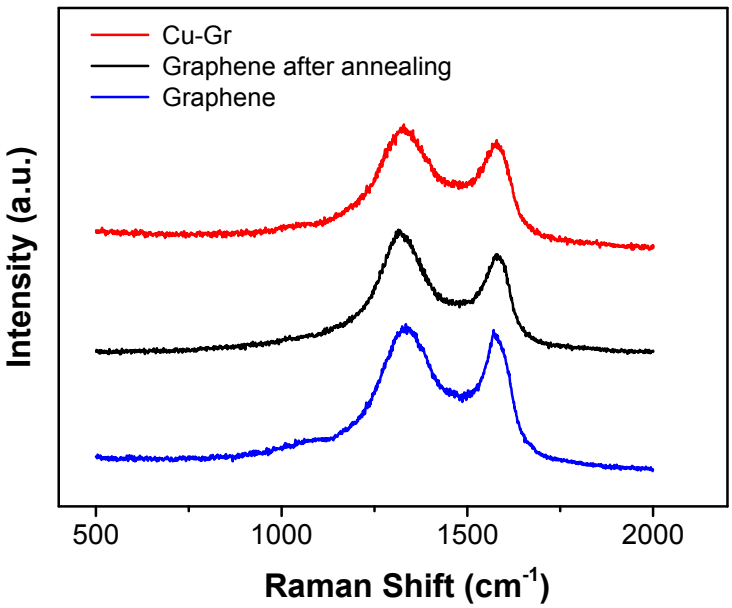

Figure S1. Raman spectra of the graphene before and after annealing in air at 300 °C, as well as the spectra of Cu-Gr.

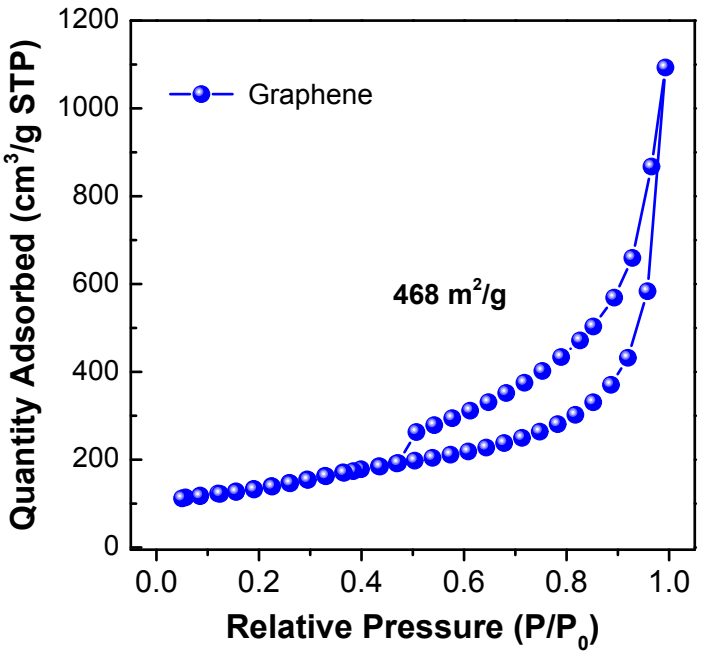

Figure S2. N_2 adsorption-desorption isotherms of graphene.

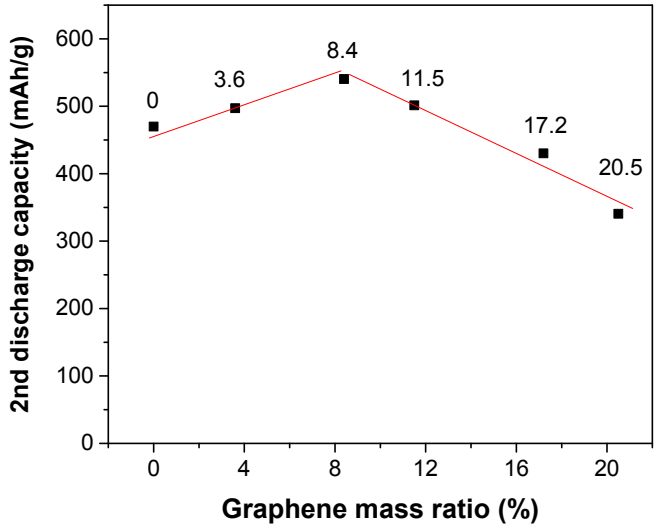

Figure S3. Materials optimization by controlling the mass ratio of graphene.

By increasing the amount of graphene from 0-8.4 wt%, the 2nd discharge capacity increases due to the well electron pathway created by graphene. Further increase from 8.4-20.5 wt% leads to the decrease of the capacity due to the reduced amount of CuO in the electrode since we are using the mass of CuO/graphene hybrids as the active materials for capacity calculation.

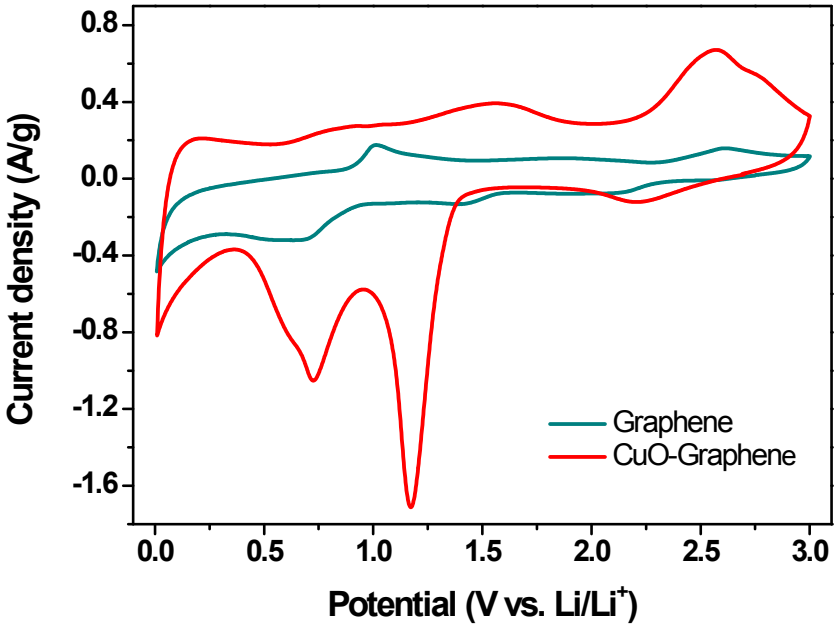

Figure S4. The 2nd cycle CV curves of pure graphene sample and CuO-Graphene hybrids at sweep rate of 0.5 mV/s in the potential window of 0.01-3.0 V vs. Li/Li^+.

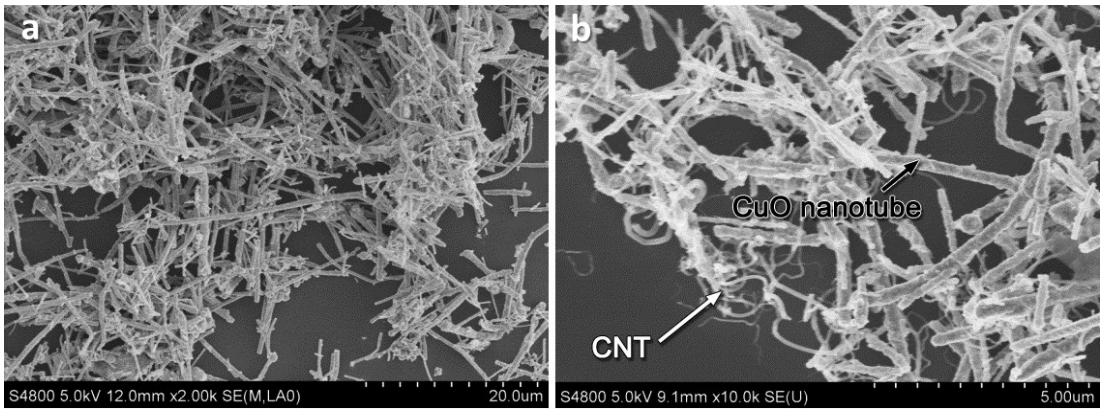

Figure S5. FESEM images of (a) CuO nanotubes and (b) CuO-CNT hybrid.

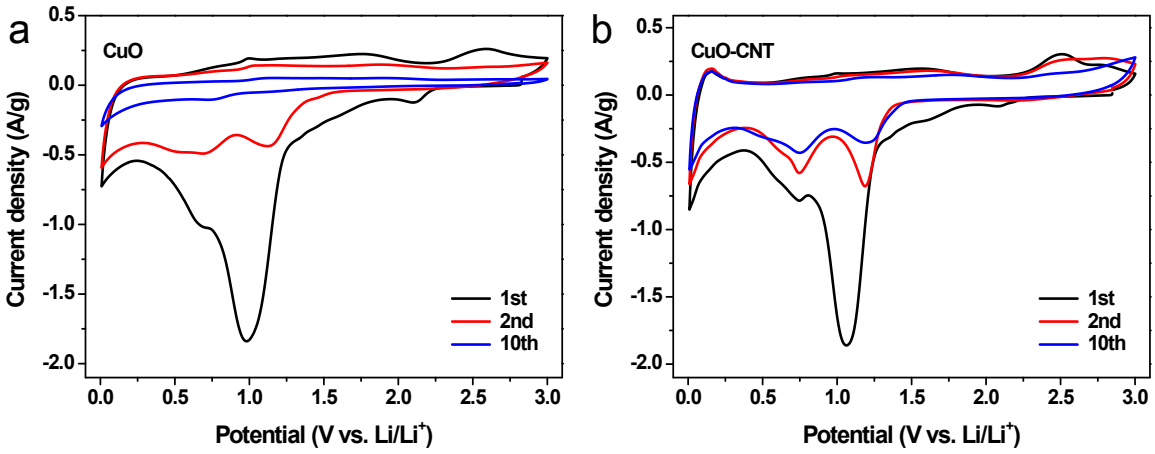

Figure S6. The 1st, 2nd and 10th cycle CV curves of CuO nanotubes and CuO-CNT hybrid.

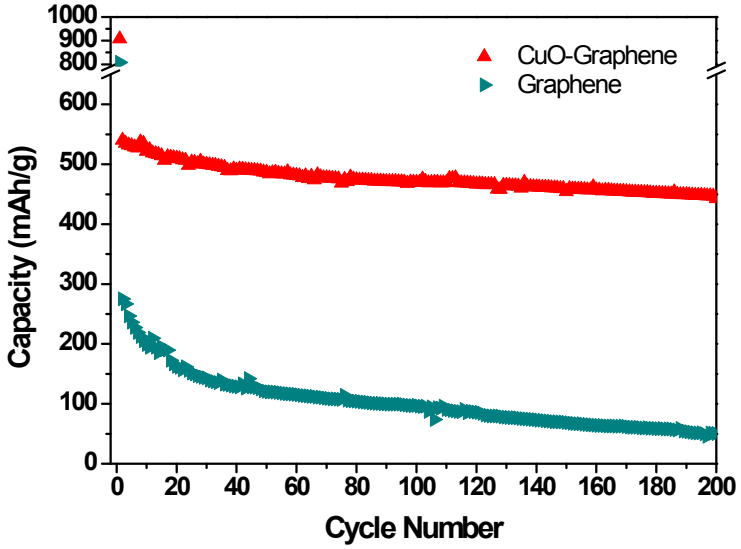

Figure S7. The long-term cycling performance at a current density of 500 mA/g for CuO-Gr and pure graphene.

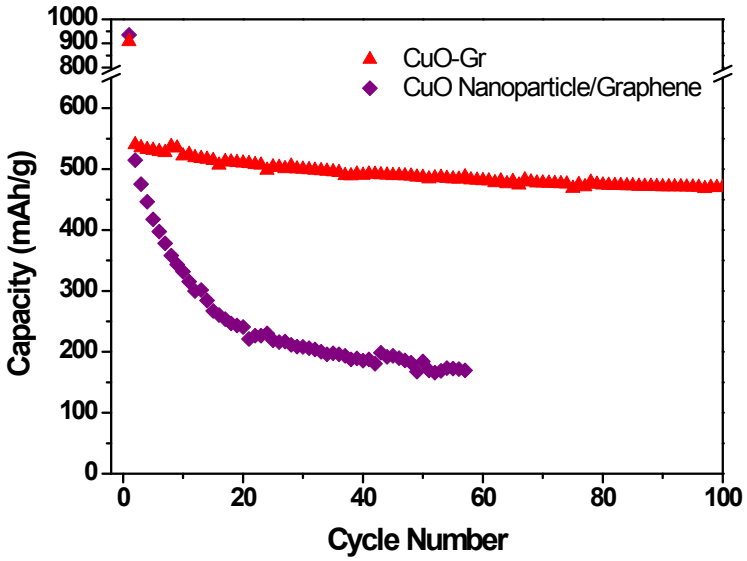

Figure S8. The long-term cycling performance at a current density of 500 mA/g for CuO-Gr and CuO nanoparticle/Graphene composite.

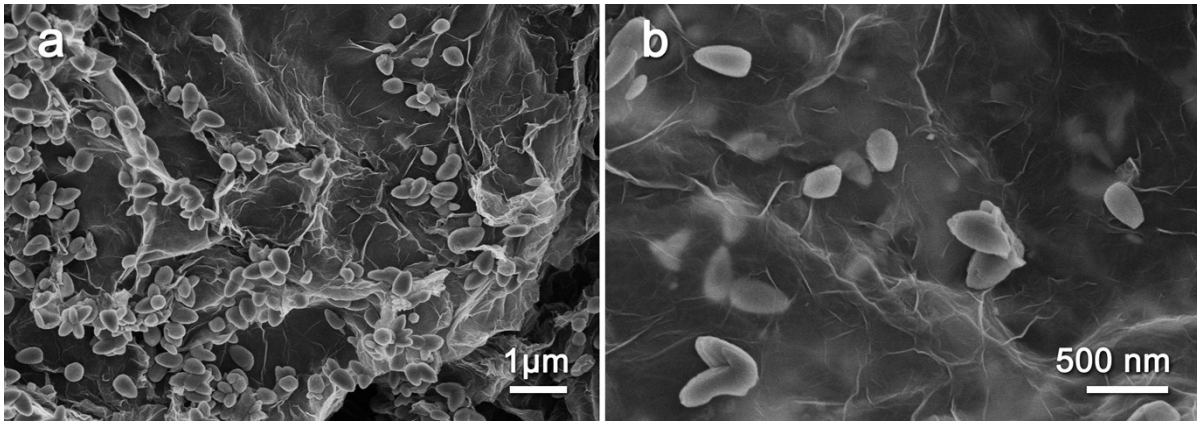

Figure S9. The SEM and high-resolution SEM images of CuO nanoparticle/Graphene composite.

Table S1. A survey of electrochemical properties of CuO-based and its hybrid composites in lithium ion batteries.

Anode materials	Potential windows (V vs. Li)	Specific capacity (mAh/g)	Cycling stability	Reference
CuO-graphene	0.01-3 V	550 mAh/g at 500 mA/g	~81 % after 250 cycles at 500 mA/g	this work
CuO-CNT	0.01-3 V	500 mAh/g at 67 mA/g	~100 % after 25 cycles at 67 mA/g	1
CuO-graphene	0.01-3 V	600 mAh/g at 65 mA/g	~100% after 100 cycles at 65 mA/g	2
CuO hollow octahedra	0.01-3 V	470 mAh/g at 100 mA/g	~87% after 100 cycles at 100 mA/g	3
CuO nanoplate	0.01-3 V	279.3 mAh/g at 670 mA/g	~ 80% after 70 cycles at 670 mA/g	4
CuO nanofiber	0.005-3 V	426 mAh/g at 100 mA/g	~94% after 100 cycles at 100 mA/g	5
CuO 3D mesocrystal	0.01-3 V	525.2 mAh/g at 67 mA/g	~100% after 500 cycles at 67 mA/g	6
CuO-graphene	0.01-3 V	736.8 mAh/g at 67 mA/g	~94.7% after 50 cycles at 67 mA/g	7
CuO-RGO	0.01-3 V	657 mAh/g at 50 mA/g	~90% after 40 cycles at 50mA/g	8

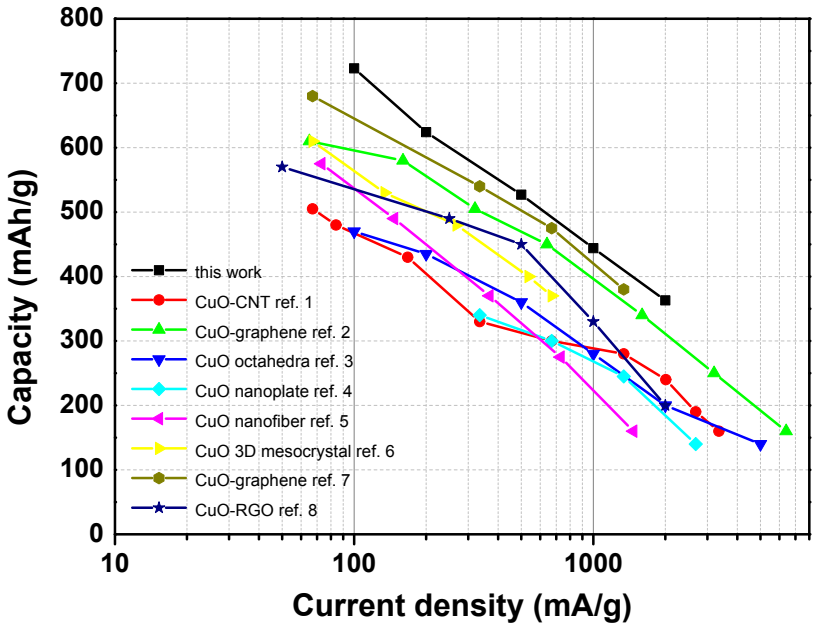

Figure S10. Rate-performance comparison of CuO-based anodes in Li-ion battery.

Reference

1. ***Chem. Mater.,*** 2008, ***20***, 3617-3622
2. ***J. Mater. Chem.,*** 2010, ***20***, 10661-10664
3. ***J. Mater. Chem. A,*** 2013, ***1***, 11126-11129
4. ***Electrochim. Acta,*** 2016, ***206***, 217-225
5. ***J. Phys. Chem. C,*** 2012, ***116***, 18087-18092
6. ***J. Mater. Chem. A,*** 2016, ***4***, 8402-8411
7. ***ACS Appl. Mater. Interfaces,*** 2013, ***5***, 9850-9855
8. ***Nano Energy,*** 2013, ***2***, 1158-1163